Chapter 9

Using Statistical Moments in Hierarchical Machine Learning for Estimation of Birefringence in Mode-Locked Fiber Laser Systems

Hasan Arda Solak[1]

Şeyma Koltuklu[2]

Sueda Turgut[3]

Mahmut Bağcı[4]

Abstract

Adaptive control and self-tuning of mode-locked fiber laser systems is an interesting topic in applied optics. Rapid and accurate detection of the cavity birefringence value is critical for the adaptive control and self-tuning of fiber laser systems. The birefringence varies randomly and significantly affects the mode-locking performance of fiber laser. In addition, the birefringence value in the laser cavity cannot be measured directly. In this study, from a new perspective, the birefringence value is determined (estimated) by hierarchical implementation of supervised machine learning algorithms. Unlike previous studies, instead of using the laser pulse energy directly, the energy evolution is recorded and a separate time series is obtained for each case of birefringence. The four statistical moments (mean, variance, skewness and kurtosis) of these time series are used as input variables (features) in the machine learning algorithm. When the findings of this study are compared

1 Marmara University, Faculty of Business Administration, Department of Management Information Systems, Türkiye

2 Marmara University, Faculty of Business Administration, Department of Management Information Systems, Türkiye

3 Marmara University, Faculty of Business Administration, Department of Management Information Systems, Türkiye

4 Marmara University, Faculty of Business Administration, Department of Management Information Systems, Türkiye

https://doi.org/10.58830/ozgur.pub865.c3507

with the results of previous studies, it is seen that the birefringence value can be estimated with higher accuracy in a short time with the hierarchical approach. More accurate classification of birefringence increases efficiency of algorithms that enable adaptive control and self-tuning of mode-locked fiber laser systems. Consequently, the study contributes to the advancement of mode-locked fiber laser technology by enhancing performance in various industrial and scientific applications, enabling broader and more efficient use of laser systems.

INTRODUCTION

Mode locking is a phenomenon frequently observed in optical resonator cavities, where nonlinear interactions in the cavity synchronize different cavity modes to generate localized and stable light pulses (Bağcı and Kutz, 2020; Bağcı and Kutz, 2022). Mode-locked fiber lasers play a crucial role in many scientific and industrial applications due to their ability to generate ultra-short pulses with high peak powers. However, the performance and stability of these systems are highly sensitive to variations in cavity birefringence, a parameter that fluctuates randomly due to environmental factors such as temperature changes or mechanical vibrations (Brunton et al., 2014). Since the birefringence value cannot be directly measured during operation, maintaining optimal performance through adaptive control and self-tuning remains a significant challenge.

Since there is the possibility of making femtosecond laser pulses with gaining media in solids, liquids, and gases, most of the time, solid-state crystal, semiconductor, or fiber materials are preferred in the construction of lasers because of their practical use. For their optical gain, these systems generally work with ion-doped insulating crystals or glasses and pump in an optical way. As soon as the ions of the gain medium absorb energy from an optical pump, these ions excite to their higher energy level and spontaneously return to the lower energy level, photon emission occurs. These photons reflect countless times between the two cavity mirrors of the laser, during which amplification of the light wave occurs. When the optical gain becomes greater than the losses such as scattering or absorption, laser light results (Sennaroğlu, 2010; Sennaroğlu, 2007).

The shortest achievable pulse duration in a laser system depends on multiple factors, including the refractive index of the material used (via the Kerr effect), nonlinear physical interactions (e.g., polarization effects, absorption, scattering), the cavity length, and the reflectivity/transmission properties of the mirrors. Achieving a stable and robust mode-locking state is particularly difficult, as minor perturbations and environmental fluctuations

can easily disrupt the cavity dispersion and destabilize the mode-locking regime (Bağcı and Kutz, 2024). The randomness of fiber setups and the environmental sensitivity of laser parameters demand specialized techniques to ensure stable operation. These systems are often modeled using nonlinear Schrödinger-type equations to capture the complex interplay of dispersion and nonlinearity in fiber cavities (Kutz, 2006).

In this context, one of the most critical parameters affecting mode-locking stability is the birefringence in the laser cavity, which effectively represents cavity-induced loss. This birefringence changes based on environmental conditions such as position, temperature, and humidity. Variations in birefringence disrupt the stability of the laser system, necessitating the continuous adjustment of filter settings to ensure consistent performance. Hence, accurate detection of birefringence changes and automated tuning of the laser cavity parameters become essential tasks for maintaining stable mode-locked operation. In existing studies, the kurtosis of the laser output signal has been used to estimate birefringence (Fu et al., 2014; Kutz and Brunton, 2015; Bağcı and Kutz, 2024).

This study presents a novel method that uses supervised machine learning algorithms to improve adaptive control and self-tuning of mode-locked fiber lasers. The suggested approach uses mean, variance, and skewness as input features in addition to kurtosis to increase the accuracy of birefringence estimation, in contrast to earlier approaches that only use kurtosis. A rich dataset is created for machine learning model training by examining the pulse energy evolution over time and identifying these four statistical moments. The classification performance and estimation speed are greatly enhanced by this method, which enables high-precision, real-time control of the laser system.

To this end, a numerical model of the fiber laser cavity is first developed, and the resulting laser output is analyzed statistically. Before applying machine learning, data preprocessing—such as normalization and cleaning—is applied to enhance model performance. Then, supervised learning algorithms including Logistic Regression, Support Vector Machines, k-Nearest Neighbors, Decision Trees, Random Forests, and Naive Bayes, are then employed and compared in terms of accuracy, precision, recall and F1-score.

NUMERICAL METHODS

Theoretical Model

In this study, the propagation of the optical field in a fiber is modeled using a coupled nonlinear Schrödinger (CNLS) equation framework (Menyuk, 1987; Menyuk, 1989).

$$i\frac{\partial u}{\partial z}+\frac{D}{2}\frac{\partial^2 u}{\partial t^2}-Ku+\left(|u|^2+A|v|^2\right)u+Bv^2u^*=iRu\,,$$

$$i\frac{\partial v}{\partial z}+\frac{D}{2}\frac{\partial^2 v}{\partial t^2}-Kv+\left(A|u|^2+|v|^2\right)v+Bu^2v^*=iRv.$$

The model describes two orthogonally polarized electric field envelopes $u(z,t)$ and $v(z,t)$ in an optical fiber. Here, t is the normalized time scaled to the pulse's full-width half-maximum, and z is the normalized propagation distance with respect to the cavity length. The components u and v represent the fast and slow polarization components, respectively (Brunton et al., 2014).

The parameter K denotes the birefringence of the cavity, while D represents the average group velocity dispersion. The parameters A and B are nonlinear coupling coefficients corresponding to cross-phase modulation and four-wave mixing, respectively. These values are determined by the physical properties of the fiber, and satisfy the condition $A + B = 1$. For a silica-based optical fiber, typical values are $A = 2/3$ and $B = 1/3$.

The terms Ru and Rv represent the gain-loss operator, incorporating the effects of Ytterbium-doped amplification, saturable gain, and bandwidth-limited amplification. The operator R is defined as:

$$R=\frac{2g_0\left(1+\tau\partial_t^2\right)}{1+\left(1/e_0\right)\int_{-\infty}^{\infty}\left(|u|^2+|v|^2\right)\mathrm{d}t}-\Gamma$$

where g_0 is the dimensionless pumping strength, and e_0 is the dimensionless saturation energy of the gain medium. The parameter τ represents the gain bandwidth, while Γ accounts for losses due to output coupling and fiber attenuation.

After each cavity round-trip, the application of wave plates and a passive polarizer is modeled via the discrete application of Jones matrices (Ding and Kutz, 2009; Komarov et al., 2005; Jones, 1941). The optical elements are defined as follows:

Quarter-wave plate:

$$W_{\lambda/4} = \begin{bmatrix} e^{-i\Pi/4} & 0 \\ 0 & e^{i\Pi/4} \end{bmatrix},$$

Half-wave plate:

$$W_{\lambda/2} = \begin{bmatrix} -i & 0 \\ 0 & i \end{bmatrix},$$

Polarizer:

$$W_p = \begin{bmatrix} 1 & 0 \\ 0 & 0 \end{bmatrix}.$$

Here, $W_{\lambda/4}$ represents the quarter-wave plate (with orientation angles α_1 and α_2), $W_{\lambda/2}$ represents the half-wave plate (with angle α_3), and W_p is the polarizer (with angle α_p). If the principal axes of these elements are not aligned with the fast axis of the cavity, a rotation matrix is applied:

$$J_j = R(\alpha_j) W_j R(-\alpha_j), R(\alpha_j) = \begin{bmatrix} \cos(\alpha_j) & -\sin(\alpha_j) \\ \sin(\alpha_j) & \cos(a_j) \end{bmatrix}$$

where α_j represents the orientation angle of each wave plate or polarizer (j = 1, 2, 3, p). These rotation angles are considered as control variables in the model and are essential for achieving mode-locking solutions. Recent experimental results have shown that these control variables can be manipulated electronically with ease, making them highly suitable for adaptive laser control systems (Shen et al., 2012).

Feature Descriptions

Input Variables

The first moment, mean, represents the average value of the laser's output power (or energy) over multiple cycles. It is used to measure the overall performance of the laser. To calculate the mean, all output energy values are summed and this total is divided by the number of measurements. Mathematically, it is expressed as:

$$\overline{x} = \frac{1}{n} \sum_{i=1}^{n} x_i$$

Here, $\overline{x}$ represents the mean output energy, x_i denotes each measurement value, and n is the number of measurements.

The variance shows the spread of output energy values around the mean. A higher variance indicates that the measurements deviate more from the mean, and thus the laser output is more unstable. The variance (s^2) is calculated as:

$$s^2 = \frac{\Sigma\left(x_i - \bar{x}\right)^2}{\left(N-1\right)}$$

Skewness indicates whether the distribution is symmetric and whether it leans to the right or left. Positive skewness suggests a longer tail on the right side, while negative skewness indicates a longer tail on the left side. Skewness (Sk) is calculated as:

$$Sk = \frac{\sum_{i=1}^{N}\left(x_i - \bar{x}\right)^3}{\left(N-1\right)s^3}$$

Kurtosis measures the extremity or the tailedness of the distribution. High kurtosis indicates more outliers in the distribution, showing greater deviations from the mean. Kurtosis ( ) is calculated as:

$$= \frac{\left(\frac{1}{n}\sum_{i=1}^{n}\left(x_i - \bar{x}\right)^4\right)}{\left(\frac{1}{n}\sum_{i=1}^{n}\left(x_i - \bar{x}\right)^2\right)^2}$$

The use of these statistical moments summarizes the dynamic behavior of the laser, offering strong and distinctive features for estimating the birefringence value (Fu et al., 2014; Kutz and Brunton, 2015).

Exploratory Data Analysis of Input Features

For generation of the sample dataset the parameters in the CNLS model are specified as follows:

D	A	B	g_0	e_0	τ	Γ
-0.4	2/3	1/3	1.73	4.23	0.1	0.1

Also, the birefringence *K* parameter is iterated between -0.32 and 0.32 with 0.01 step size, while the polarizer angle (α_p) is varying from -90° to 90° with 1° of step size. Thus, the number of instances of training sample dataset is 65x181=11765. To test the machine learning models, we generated a separate mis-aligned (noised) dataset in which we have 1000 instances with random K and α_p values.

To gain a better understanding of the dataset's underlying structure, the distributions of all input features were examined before the model was trained. Every input variable displays a unique statistical pattern, as shown in **Figure 1**.

The intricacy and non-linearity of the birefringence estimation task are revealed by these visualizations' features. Additionally, they defend the use of tree-based models, like Random Forests, which don't require rigid parametric assumptions and are ideal for handling skewed and non-normally distributed data.

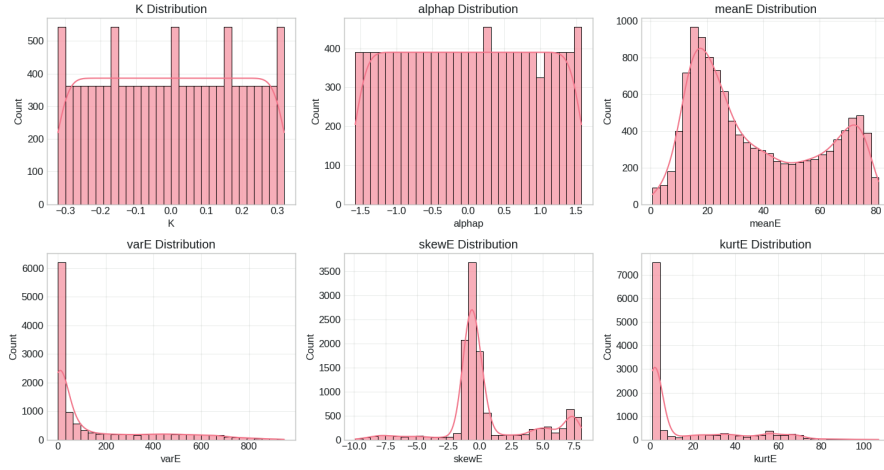

Figure 1. Histogram of all input features used in the model. The figure highlights the statistical characteristics and potential skewness of each feature distribution.

Supervised Machine Learning Methods

In recent years, machine learning algorithms and artificial intelligence techniques have been extensively employed to enhance the functionality and performance of mode-locked fiber lasers (Bağcı and Kutz, 2024). In particular, Artificial Neural Networks (ANNs) have been utilized to improve system architecture, operational efficiency, and control mechanisms. These

methods have also demonstrated notable success in areas such as signal processing, system modeling, channel equalization, and the efficient control of optical systems (Freire et al., 2023; Ma et al., 2022; Mezzi et al., 2023; Boscolo and Finot, 2020). Additionally, Genetic Algorithms (GAs) have been adopted to fully automate the startup procedures of laser systems, thereby contributing to enhanced reliability and operational efficiency (Ma et al., 2022; Han et al., 2024; Woodward and Kelleher, 2016).

In the present study, six supervised machine learning algorithms are employed, including Logistic Regression (LR), Support Vector Machines (SVM), K-Nearest Neighbors (KNN), Decision Trees (DT), Random Forests (RF), and Naive Bayes (NB).

Logistic Regression (LR) is a widely used method for binary classification tasks. This supervised learning technique models a binary outcome variable using an S-shaped logistic (sigmoid) function (Tolles, 2016). Through this function, LR defines decision boundaries between classes, which may range from simple linear to complex nonlinear structures depending on the nature of the classification problem (Gudivada et al., 2016; DeMaris, 1995).

Support Vector Machines (SVM) are supervised algorithms applicable to both classification and regression problems. This method separates data points into different classes using a hyperplane that maximizes the margin between classes (Vapnik and Cortes, 1995; Burges, 1998). Data points closest to the hyperplane, known as support vectors, are critical to defining the decision boundary. In the context of mode-locked fiber lasers, SVMs have been effectively used to analyze cavity parameter spaces essential for achieving stable mode-locking.

K-Nearest Neighbors (KNN) is a non-parametric, instance-based learning algorithm that can be applied to both classification and regression problems. One of the key advantages of KNN is the absence of a training phase; instead, it assigns class labels based on similarity metrics—such as Euclidean or Manhattan distance—to the nearest neighbors in the feature space (Cover, 1967; Hall et al., 2008; Keller et al., 1985). Although computationally intensive, KNN is particularly effective in scenarios where data are balanced and class boundaries are not well defined.

Decision Trees (DT) represent a non-parametric supervised learning approach that uses a hierarchical tree structure to model decisions based on input features (Twa et al., 2005; Rokach, 2014; Brodley and Utgoff, 1995). The algorithm sequentially partitions the input space and assigns class labels based on impurity measures such as Gini index or entropy (Quinlan, 1986).

DTs are especially effective in large and complex datasets for uncovering meaningful patterns and identifying influential features (Myles et al., 2004).

Random Forest (RF) is an ensemble-based supervised learning algorithm designed for both classification and regression tasks. It consists of multiple decision trees constructed with random subsets of the training data and features. The ensemble nature of RF helps mitigate overfitting and improves generalization performance by averaging predictions from multiple models (Breiman, 2001; Schonlau and Zou, 2020; Ho, 1995). RF is known for its robustness and scalability, making it well-suited for high-dimensional and large-scale datasets (Paul et al., 2018).

Naive Bayes (NB) is a probabilistic classification algorithm grounded in Bayes' theorem. It operates under the assumption of conditional independence among input features (Bernardo and Smith, 2001). NB computes the posterior probabilities of each class and assigns the class label with the highest probability using maximum likelihood estimation (Hastie et al., 2001). Despite its simplicity and strong independence assumption, Naive Bayes remains a highly effective model, particularly in large-scale and high-dimensional problems due to its computational efficiency.

Model Training and Validation

Model Training

The selected supervised machine learning algorithms were trained on the training dataset to estimate the birefringence value. The training process involves the model learning the relationships between the input variables (statistical moments) and the output variable (birefringence value). During this stage, the model's parameters are optimized to minimize the error on the training data.

Grid Search-Based Hyperparameter Optimization

To ensure optimal model performance in birefringence estimation, a systematic hyperparameter tuning process was applied to the Random Forest algorithm. A grid search strategy combined with five-fold cross-validation was employed to explore a wide range of parameter combinations. This procedure involved evaluating 432 distinct configurations across multiple decision trees, resulting in a total of 2160 model fits.

The hyperparameters considered in this optimization included the number of trees in the forest, maximum tree depth, the minimum number of samples required to split an internal node, the minimum number of samples required to be at a leaf node, the method used to select the number

of features at each split, and class weight adjustments to handle potential class imbalances.

Following this exhaustive search, the configuration that achieved the highest cross-validated accuracy was selected as the optimal model setup. This final set of parameters enhanced the model's ability to generalize across different birefringence levels and contributed significantly to the overall robustness and precision of the classification results.

Metrics for Performance Measurement

The performance of the trained model was evaluated on the validation dataset using various metrics. These metrics provide comprehensive information about the accuracy and reliability of the model's predictions.

Accuracy: The ratio of correctly predicted instances to the total number of instances. It is a general indicator of overall performance and can be sufficient on its own, especially for balanced datasets.

Precision: Indicates how many of the instances predicted as positive by the model are actually positive. It is important for minimizing false positives. For instance, in critical laser systems, the cost of a false positive alarm can be high.

Recall: Shows how many of the actual positive instances were correctly identified as positive by the model. It is important for minimizing false negatives. This metric is crucial because the failure to correctly identify the birefringence value can lead to unstable laser system operation.

F1-score: The harmonic mean of precision and recall. It provides a more informative performance measure than accuracy alone, especially in unbalanced datasets.

RESULTS

Running multiple classification models on the birefringence dataset yielded insightful comparative results regarding their segmentation capability. As illustrated in **Figure 2**, all models performed above a moderate threshold; however, their success varied significantly. Among the tested algorithms, Random Forest and Decision Tree achieved the highest accuracy—approaching 0.99 across all evaluated metrics, including precision, recall, and F1-score. In contrast, traditional methods such as Naive Bayes and Logistic Regression showed noticeably lower performance, with accuracies around 0.55 and 0.53, respectively. This clear distinction highlights the superior ability of tree-based ensemble methods in capturing the nonlinear and statistical characteristics of birefringence dynamics.

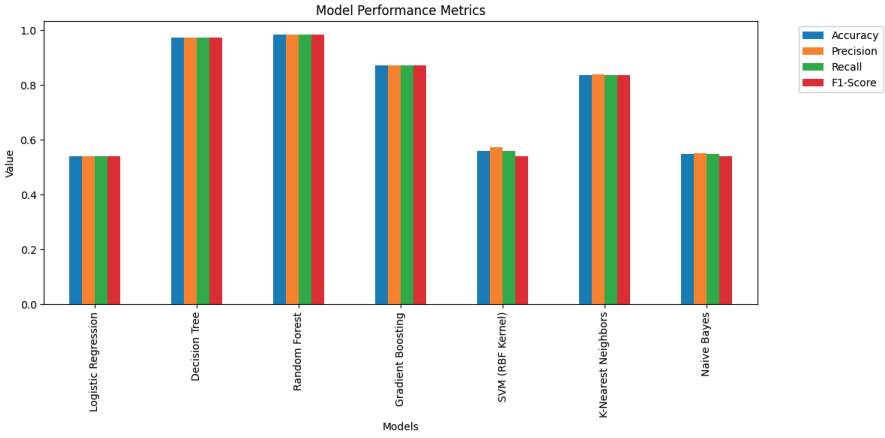

Figure 2. Comparison of classification performance metrics (Accuracy, Precision, Recall, F1-Score) across supervised machine learning models used for birefringence level prediction.

Following the comparative evaluation, the Random Forest classifier was selected for hierarchical classification due to its balance of interpretability, scalability, and strong empirical performance. To assess its robustness under different iterations, the continuous K values are discretized (classified) into 2 to 32 levels using quantile-based binning.

Figure 3 presents the accuracy trends across the number of iterations (hierarchically). The model achieved 98.9% accuracy for (2^1)-class (or two-class) classification, and despite a gradual decline in performance with increasing iteration number, the model retained strong accuracy (88.2%) even at (2^5)-class (or 32-class) classification. The decline is expected due to the increased complexity and reduced separation between classes in higher-resolution binning.

Furthermore, a summary of performance metrics is shown in **Table 1**, where precision, recall, and F1-score values remain highly consistent with overall accuracy. All scores remained above 0.88, validating the model's reliability across both coarse and fine classifications.

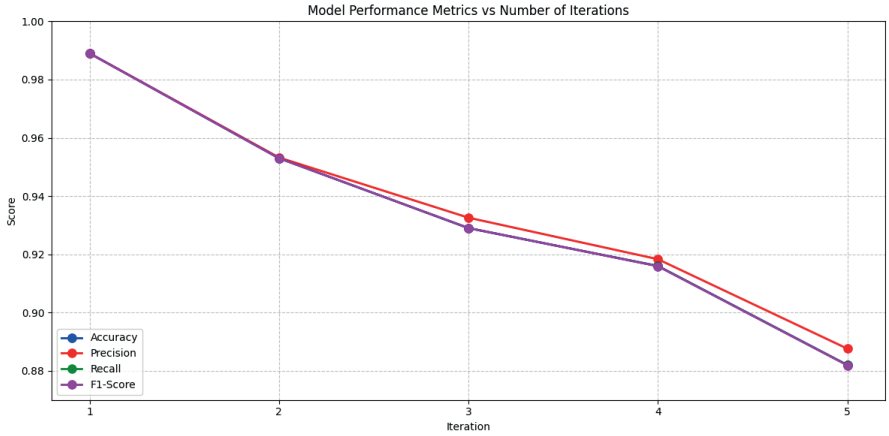

Figure 3. Accuracy, precision, recall, and F1-score trends of the Random Forest model across different birefringence classification levels (number of iterations).

Table 1. Performance metrics (accuracy, precision, recall, and F1-score) of the Random Forest classifier for different iterations.

Iteration	Performance Metrics			
	Accuracy	Precision	Recall	F1-Score
1	0.9890	0.9890	0.9890	0.9890
2	0.9530	0.9532	0.9530	0.9530
3	0.9290	0.9326	0.9290	0.9290
4	0.9160	0.9183	0.9160	0.9159
5	0.8820	0.8876	0.8820	0.8819

To better understand the internal decision-making process of the Random Forest classifier, a feature importance analysis is performed. As illustrated in **Figure 4**, the polarizer angle (α_p) emerges as the most significant contributor to model performance, followed by higher-order statistical moments such as skewness and kurtosis.

DISCUSSION AND CONCLUSION

Using polarizer angle and statistical moments of the energy evolution as inputs, the study's findings showed how well a hierarchical machine learning technique estimates birefringence in mode-locked fiber laser systems. With accuracy values above 92% in low-resolution class definitions, Random Forest performed noticeably better than the other classifiers that were

evaluated. This lends credence to the claim that complex and nonlinear optical dynamics were best handled by ensemble-based decision models.

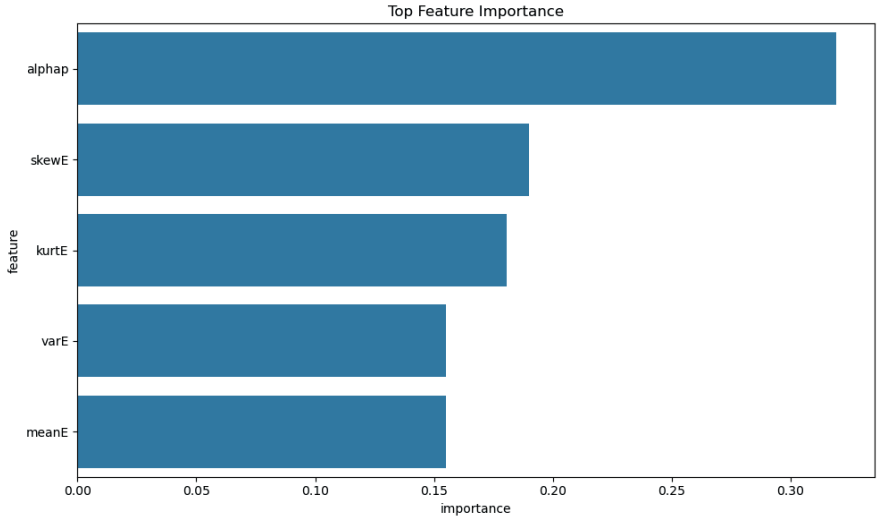

Figure 4. Relative importance of input features in the Random Forest model for birefringence classification. The polarizer angle (α_p) dominates in importance, followed by skewness (skewE), kurtosis (kurtE), variance (varE), and mean (meanE).

While a previous study employing sparse representation techniques under misalignment reported an accuracy of 88% (Fu et al., 2014), our method achieved a comparable level of accuracy while offering greater robustness in multi-level classification scenarios. Moreover, the present study eliminates the need for alignment-dependent spectrogram inputs by directly utilizing time-domain statistical features. This methodological distinction provides advantages in terms of both computational efficiency and implementation flexibility for real-world laser control applications.

The consistent performance across all levels of classification indicates the reliability of moment-based features in capturing essential variations in the laser cavity. In particular, skewness and kurtosis—higher-order statistical measures—proved highly discriminative, confirming that birefringence states influence the asymmetry and tailedness of the energy evolution data. The use of the polarizer angle (α_p) as an input also adds to the model's predictive power while preserving its independence from physical modeling constraints.

In practical terms, this work aids in the creation of adaptive laser control real-time birefringence recognition systems. Accurate and quick birefringence detection can increase laser systems' self-tuning capabilities, shorten maintenance schedules, and boost long-term operational effectiveness. Furthermore, the model's ability to scale to higher resolution levels raises the possibility of its incorporation into more intricate fiber laser networks or multi-NPR (nonlinear polarization rotation) setups.

In conclusion, a very precise, understandable, and ready-to-implement solution for birefringence classification in fiber laser systems was provided by the hierarchical Random Forest classifier trained on moment-based features. Future research might examine hybrid models that combine spectral and statistical features for even greater precision, real-time deployment, or transfer learning across various laser architectures.

References

Bağcı M, Kutz JN, 2020. Spatiotemporal mode locking in quadratic nonlinear media. Phys. Rev. E 102(9), 022205.

Bağcı M, Kutz JN, 2022. Mode-locking in quadratically nonlinear waveguide arrays. Opt. Express 30, 28454-28469.

Bağcı M, Kutz N, 2024. Machine learning for self-tuning mode-locked lasers with multiple transmission filters. Optical Society, 79–89.

Bernardo JM, Smith AFM, 2001. *Bayesian theory*. Measurement Science and Technology, vol. 12, pp. 221–222.

Boscolo S, Finot C, 2020. Artificial neural networks for nonlinear pulse shaping in optical fibers. Optics & Laser Technology, 131: 106446.

Breiman L, 2001. Random forests. Machine Learning, 4: 5–32.

Brodley C, Utgoff P, 1995. Multivariate decision trees. Machine Learning, 19: 45–77.

Burges CJ, 1998. A Tutorial on Support Vector Machines for Pattern Recognition. Data Mining and Knowledge Discovery, 2: 121–167.

Cover PHT, 1967. Nearest neighbor pattern classification. IEEE Transactions on Information Theory, 13(11): 21–27.

DeMaris A, 1995. A Tutorial in Logistic Regression. Journal of Marriage and Family, 57(14): 956–968.

Ding E, Kutz JN, 2009. Operating regimes, split-step modeling, and the Haus master mode-locking model. Journal of the Optical Society of America B, 26(11): 2290–2300.

Freire P, Manuylovich E, Prilepsky JE, Turitsyn SK, 2023. Artificial neural networks for photonic applications—from algorithms to implementation: tutorial. Advances in Optics and Photonics, 15: 739–834.

Fu X, Brunton SL, Kutz JN, 2014. Classification of birefringence in mode-locked fiber lasers using machine learning and sparse representation. Optics Express, 22(7): 8585–8597.

Gudivada VN, Irfan MT, Fathi E, Rao DL, 2016. Cognitive analytics: Going beyond big data analytics and machine learning. In: Bhatnagar R, Srinivasan K (Editors), Cognitive Computing: Theory and Applications. Elsevier, pp. 169–205, Amsterdam – Netherlands.

Han D, Guo R, Li G, Chen Y, Zhang B, Ren K, Zheng Y, Zhu L, Li T, Hui Z, 2024. Automatic mode-locked fiber laser based on adaptive genetic algorithm. Optical Fiber Technology, 83.

Hall P, Park BU, Samworth RJ, 2008. Choice of neighbor order in nearest-neighbor classification. The Annals of Statistics, 36(15): 2135–2152.

Hastie T, Tibshirani R, Friedman JH, 2001. *The Elements of Statistical Learning: Data Mining Inference and Prediction.* Springer, New York – USA.

Jones RC, 1941. A new calculus for the treatment of optical systems. I. Description and discussion of the calculus. Journal of the Optical Society of America, 31(7): 488–493.

Keller JM, Gray MR, Givens JA, 1985. A fuzzy k-nearest neighbor algorithm. IEEE Transactions on Systems, Man, and Cybernetics, 14: 580–585.

Komarov A, Leblond H, Sanchez F, 2005. Multistability and hysteresis phenomena in passively mode-locked fiber lasers. Physical Review A, 71: 053809.

Kutz JN, 2006. Mode-locked soliton lasers. SIAM Review, 48(4): 629–678.

Ma X, Lin J, Dai C, Lv J, Yao P, Xu L, Gu C, 2022. Machine learning method for calculating mode-locking performance of linear cavity fiber lasers. Optics & Laser Technology, 149.

Ma X, Lv J, Luo J, Liu X, Yao P, Xu L, 2023. Pulse convergence analysis and pulse information calculation of NOLM fiber mode-locked lasers based on machine learning method. Optics & Laser Technology, 163.

Menyuk CR, 1987. Nonlinear pulse propagation in birefringent optical fibers. IEEE Journal of Quantum Electronics, 23(2): 174–176.

Menyuk CR, 1989. Pulse propagation in an elliptically birefringent Kerr medium. IEEE Journal of Quantum Electronics, 25(12): 2674–2682.

Mezzi R, Bahloul F, Karar AS, Ghandour R, Salhi M, 2023. Predicting behavior of photonic crystal fiber lasers using artificial neural networks. Optics Communications, 542.

Myles AJ, Feudale RN, Liu Y, Woody NA, Brown SD, 2004. An introduction to decision tree modeling. Journal of Chemometrics, 18(16): 275–285.

Paul A, Mukherjee DP, Das P, Gangopadhyay A, Chintha AR, Kundu S, 2018. Improved random forest for classification. IEEE Transactions on Image Processing, 27(18): 4012–4024.

Rokach L, 2014. *Data Mining with Decision Trees.* World Scientific Pub. Co. Inc., Singapore.

Quinlan R, 1986. Induction of decision trees. Machine Learning, 1: 81–106.

Schonlau M, Zou RY, 2020. The random forest algorithm for statistical learning. The Stata Journal, 20(11): 3–29.

Sennaroğlu A, 2007. Fotonik ve katıhal lazerleri. Bilim ve Teknik, 40–46.

Sennaroğlu A, 2010. Katıhal femtosaniye lazerleri. Bilim ve Teknik, 48–53.

Shen X, Li W, Yan M, Zeng H, 2012. Electronic control of nonlinear-polarization rotation mode locking in Yb-doped fiber lasers. Optics Letters, 37: 3426–3428.

Tolles WJM, 2016. Logistic regression: Relating patient characteristics to outcomes. Journal of the American Medical Association, 316(15): 533–534.

Twa MD, Parthasarathy S, Roberts CJ, Mahmoud AM, Raasch TW, Bullimore MA, 2005. Automated decision tree classification of corneal shape. Optometry and Vision Science, 82: 1038–1046.

Vapnik V, Cortes C, 1995. Support-vector networks. Machine Learning, 20: 273–297.

Woodward RI, Kelleher EJR, 2016. Towards 'smart lasers': Self-optimisation of an ultrafast pulse source using a genetic algorithm. Scientific Reports, 6: 37616.

Acknowledgment

This research was supported by the Scientific and Technological Research Council of Türkiye (TÜBİTAK) under the 2209-A University Students Research Projects Support Program, with the grant number 1919B012414330.

Conflict of Interest

The authors have declared that there is no conflict of interest.